Development 130, 3015-3026

doi:10.1242/dev.00488

pannier and *pointedP2* act sequentially to regulate *Drosophila* heart development

Alejandra D. Alvarez[1], Weiyang Shi[2], Beth A. Wilson[1] and James B. Skeath[1,*]

[1]Department of Genetics, Washington University School of Medicine, 4566 Scott Avenue, St Louis, MO 63110, USA
[2]Program in Developmental Biology, Washington University School of Medicine, 4566 Scott Avenue, St Louis, MO 63110, USA
*Author for correspondence (email: jskeath@genetics.wustl.edu)

Accepted 17 March 2003

SUMMARY

The *Drosophila* heart consists of two major cell types: cardioblasts, which form the contractile tube of the heart; and pericardial cells, which flank the cardioblasts and are thought to filter and detoxify the blood or hemolymph of the fly. We present the completion of the entire cell lineage of all heart cells. Notably, we detect a previously unappreciated distinction between the lineages of heart cells located in the posterior seven segments relative to those located more anteriorly. Using a genetic screen, we have identified the ETS-transcription factor *pointed* as a key regulator of cardioblast and pericardial cell fates in the posterior seven segments of the heart. In this domain, *pointed* promotes pericardial cell development and opposes cardioblast development. We find that this function of *pointed* is carried out primarily if not exclusively by the *pointedP2* isoform and, that in this context, *pointedP2* may act independently of Ras/MAPK pathway activity. We go on to show that the GATA transcription factor *pannier* acts early in dorsal mesoderm development to promote the development of the cardiac mesoderm and thus all heart cells. Finally, we demonstrate that *pannier* acts upstream of *pointed* in a developmental pathway in which *pannier* promotes cardiac mesoderm formation, and *pointed* acts subsequently in this domain to distinguish between cardioblast and pericardial cell fates.

Key words: *Drosophila*, Heart development, GATA factor, ETS-domain proteins

INTRODUCTION

Comparative studies between vertebrates and *Drosophila* highlight a significant conservation in the embryology and molecular regulation of heart development (reviewed by Bodmer and Frasch, 1999; Cripps and Olson, 2002). For example, in *Drosophila* and vertebrates the heart develops from those mesodermal cells that migrate most distally from the original point of invagination during gastrulation. In addition, the mature *Drosophila* heart is a simple linear tube and resembles the primitive heart tube of vertebrates prior to the processes of looping and septation that ultimately create a multi-chambered heart. Furthermore, molecular studies indicate that similar gene cassettes govern heart formation in *Drosophila* and vertebrates. The homeodomain gene *tinman* (*tin*) and the GATA transcription factor *pannier* (*pnr*) are necessary for heart formation in *Drosophila*. Similarly, transcription factors of the Tin and GATA families are also essential for vertebrate heart formation. In both *Drosophila* and vertebrates, the BMP signaling pathway controls the proper establishment of the expression profiles of Tin and GATA family members in the heart primordium. Thus, *Drosophila* provides an excellent model for early heart development. Despite this, we know little about the genetic regulatory mechanisms that specify the individual cell types of the *Drosophila* heart and we lack a complete knowledge of the lineal relationships of all heart cells.

The *Drosophila* heart is composed of two cell types (reviewed by Bodmer and Frasch, 1999). Cardioblasts express muscle-specific proteins, coalesce to form the linear heart tube and are the contractile cells of the heart. Pericardial cells are loosely associated with and flank the cardioblasts; these cells do not express muscle specific proteins and are thought to filter and detoxify the blood or hemolymph of the fly. Cardioblasts and pericardial cells develop from closely interspersed precursor cells that develop in the dorsalmost region of the mesoderm, termed the cardiac mesoderm. After precursor divisions, heart cells on both sides of the embryo align themselves into two rows of cells, with pericardial cells being displaced slightly ventral and interior to the tightly aligned row of cardioblasts at the dorsalmost extent of the mesoderm. As dorsal closure occurs, the bilaterally symmetric rows of heart cells move toward each other and the two rows of cardioblasts meet at the dorsal midline, align perfectly with one another and coalesce to form a lumen between them. Subsequently, the heart tube becomes divided into two domains: the aorta more anteriorly and the heart proper in the posterior three segments. The heart proper is distinguished from the aorta by a wider bore and the presence at segmental intervals of ostia, the inflow valves of the heart. Here, we collectively refer to the aorta and heart proper as the heart.

Gene expression, cell lineage and morphological studies indicate that distinct subtypes of cardioblasts and pericardial cells populate the heart (see Fig. 7) (Gajewski et al., 2000; Jagla et al., 1997; Lo and Frasch, 2001; Lo et al., 2002; Ward and Skeath, 2000). These studies also distinguish the development and gene expression profiles of heart cells located in the posterior seven segments relative to those found more anteriorly. Each hemisegment of the posterior region contains six cardioblasts and ten pericardial cells. Cardioblasts can be roughly divided into two classes: those that express Svp but not Tin (these are the first two cardioblasts of a hemisegment); and those that express Tin but not Svp, the four remaining cardioblasts of a hemisegment. The lineage of these cardioblasts is known and shown in Fig. 7. Pericardial cells can be divided into three classes: Eve-, Tin- and Odd-positive pericardial cells. The relative position of these cells is shown in Fig. 7. The cell lineage of the Odd-positive pericardial cells is known; however, the lineage of Eve- and Tin-positive pericardial cells remains unclear.

In contrast to the posterior region, all 12 cardioblasts that develop anterior to this domain express Tin but not Svp. In this region, Eve- and Tin-positive pericardial cells develop normally, while Odd-positive pericardial cells are replaced by Odd-expressing lymph gland cells. The differences in gene expression between heart cell types in the same region as well as between different anteroposterior (AP) regions suggest functional specialization of cardioblasts and pericardial cells both within the same region and between different AP regions. Consistent with this model, the Svp-cardioblasts in the posterior three heart segments form the ostia of the larval heart (Molina and Cripps, 2001).

Genetic studies have identified the Nk2 type homeodomain protein Tin as a key regulator of heart development (reviewed by Bodmer and Frasch, 1999; Cripps and Olson, 2002). *tin* expression is the earliest known marker of the cardiac mesoderm and loss-of-function mutations in *tin* result in the complete absence of all heart cells, as well as all other dorsal mesodermal derivatives. In addition to *tin*, heart cell development absolutely requires the function of the AP patterning genes *wingless* and *sloppy-paired*. Despite the identification of a number of genes required to promote the development of all heart cells, very few genes have been identified that regulate the decision of cells to choose between the cardioblast and pericardial cell fate. One such gene appears to be the GATA zinc-finger transcription factor *pnr* (Ramain et al., 1993). Loss of *pnr* function results in a significant loss of cardioblasts and an apparent increase in at least one class of pericardial cells, the Eve-positive pericardial cells (Gajewski et al., 1999). Other genes are likely to act with or in opposition to *pnr* to regulate the decision of cells to acquire the cardioblast or pericardial cell fate.

The *pointed* (*pnt*) locus encodes two protein isoforms, both of which act as transcriptional effectors of the Ras/MAP-kinase pathway (Brunner et al., 1994; Klaes et al., 1994; Klambt, 1993; O'Neill et al., 1994). The two Pnt isoforms, PntP1 and PntP2, are members of the ETS family of transcription factors and arise due to alternative use of two promoters separated by roughly 50 kb. PntP1 and PntP2 contain unique domains at their N terminus but share the identical stretch of 394 amino acids at their C terminus within which resides the ETS DNA-binding domain. The DNA-binding properties of these proteins appear identical; however, PntP1 and PntP2 exhibit crucial differences in their functional properties and transcriptional regulation. PntP1 is a constitutive transcriptional activator and Ras/MAP-kinase pathway activity induces PntP1 transcription (Gabay et al., 1996). By contrast, PntP2 is not a constitutive transcriptional activator and *pntP2* transcription appears to be independent of Ras/MAP-kinase activity. Nonetheless, PntP2 activity depends on Ras/MAP kinase activity as Ras/MAP kinase-mediated phosphorylation of PntP2 at Thr151 turns it into a potent transcriptional activator (Brunner et al., 1994; O'Neill et al., 1994). Although PntP1 and activated PntP2 regulate the development of many different cell types and tissues in *Drosophila*, a role for *pnt* function in cardioblast development has not been identified.

We present evidence that *pnt* plays a region specific role in regulating cardioblast and pericardial cell development. Loss of *pnt* function results in an approximate twofold increase in cardioblasts and an almost commensurate decrease in pericardial cells. This increase in cardioblasts arises largely from a specific increase in Svp-positive cardioblasts and is restricted to the posterior seven heart segments where Svp-positive cardioblasts normally develop. We demonstrate that this effect of *pnt* is carried out primarily if not exclusively by the PntP2 isoform, and that in this context PntP2 may act independently of Ras/MAP kinase pathway activity. Contrary to a prior study, we find that *pnr* acts early in mesoderm development to promote the development of the cardiac mesoderm and thus the development of all heart cells. Phenotypic analyses of *pnr pnt* double mutant embryos suggest a model whereby *pnr* acts before *pnt* to promote the formation of the cardiac mesoderm and that *pnt* acts subsequently within this domain to distinguish between cardioblast and pericardial cell fates. In addition, we present the completion of the cell lineage of all heart cells. These pedigree analyses identify a clear distinction between the lineage of anterior cardioblast and those that develop in the posterior seven segments. The transition point between these heart cell lineages correlates perfectly with the region specific effect of *pnt* on heart development. These results suggest independent genetic control of heart cell development in the anteriormost region of the heart relative to the posterior seven segments.

MATERIALS AND METHODS

Fly strains and genetics

Wild-type patterns of gene expression were examined in Oregon R embryos. Fly lines used include $pnt^{S012309}$, pnt^{2}, pnt^{RM254}, $pnt^{\Delta 88}$, pnt^{RR112}, pnr^{1}, pnr^{VX6}, spi^{IIA}, $Star^{IIN}$, $rhomboid^{del-1}$, aop^{1}, $heartless^{AB42}$, $aos^{\Delta 7}$, $vein^{Ry}$, $vein^{\gamma 3}$, $heartbroken^{ems6}$ and svp^{H162}. svp^{H162} is an enhancer trap insert in svp and is referred to as *Svp-lacZ* (Mlodzik et al., 1990). Gene misexpression was achieved with the Gal4-UAS system and the following lines: Twi-GAL4, UAS-DNEgfr, UAS-DN-heartless, UAS-DNras, UAS-pntP1 and UAS-pntP2. Standard genetic crosses were used to create the multiply mutant fly lines noted in the text.

Lineage-tracing experiments

Random *lacZ*-expressing clones were created using the FLP/FRT lineage tracing system as described previously (Ward and Skeath, 2000) with the following modifications. Three- to four-hour-old embryos of the appropriate genotype were heat-shocked for 20

minutes at 33°C to induce *flp* recombinase, placed at 18°C and aged until stage 15-16, at which point they were fixed and stained.

Antibody generation and immunohistochemistry and immunofluorescence

Amino acids 1-230 of PntP1 were cloned into pET (Novagen) for protein expression and purification. This protein domain is unique to PntP1. This antigen was used to immunize rabbits at Pocono Rabbit Farm. The PntP1 antibody is specific for PntP1 because it detects a protein expressed in a pattern identical to *pntP1* RNA and because the antibody does not detect antigen in embryos that delete the *pntP1*-specific exons and downstream exons of the *pnt* locus.

Single- and double-label immunohistochemistry analyses were performed as described previously (Skeath, 1998). We used the following antibodies at the indicated dilutions: mouse anti-Zfh1 (1:1000) (Lai et al., 1991); rabbit anti-Mef2 (1:1000) (Lilly et al., 1995); rabbit anti-Eve (1:2000) (Frasch et al., 1987); mouse anti-β-gal (1:2000; Promega); rabbit anti-β-gal (1:2000; Jackson); rabbit anti-Tin (1:500) (Azpiazu and Frasch, 1993); rabbit anti-Pnr (1:400) (Herranz and Morata, 2001); rabbit anti-Odd (1:500) (Ward and Skeath, 2000); rabbit anti-PntP1 (1:500).

Double stranded RNA interference (dsRNAi) and allele sequencing

RNAi was prepared as described previously (Kennerdell and Carthew, 1998). We used dsRNA probes specific for *pntP1* or *pntP2* to target each isoform independently. For *pntP1* we made dsRNA corresponding to nucleotides 1-690 of the *pntP1*-coding region. This region encodes for the entire *pntP1*-specific domain. For *pntP2*, we made dsRNA for corresponding to nucleotides 1-906 of the *pntP2* coding region. This region encodes ~90% of the *pntP2*-specific domain. dsRNA was injected into the posterior region of pre-cellular blastoderm embryos at a concentration of 2 μg/μl, and the embryos were allowed to develop until stage 15 to 16 at which point embryos were collected and fixed for immunohistochemistry.

We identified the molecular lesions in pnt^{2}, pnt^{RR112} and pnr^{1} by PCR-based sequencing of the entire coding region and intron/exon boundaries of the appropriate locus from genomic DNA obtained from each mutant background. pnt^{2} contains G to A conversion at base 2653 of the *pntP1* cDNA (base 2667 of the *pntP2* cDNA) (Klambt, 1993). This mutation converts the tryptophan (W) at amino acid 536 of PntP1 (amino acid 631 of PntP2) to a premature stop codon, truncating both PntP1 and PntP2 roughly one third of the way through the shared ETS-DNA-binding domain. pnt^{RR112} contains a G to A conversion in the splice donor site of exon IV in *pntP2*. This lesion converts the GT donor site to AT, and is expected to disrupt splicing of *pntP2* but not *pntP1* because this exon is specific for *pntP2*. pnr^{1} contains a G to A conversion at nucleotide 1034. This mutation converts a W to a premature stop codon, truncating the *pnr* midway through the first zinc finger.

RESULTS

Completion of the cell lineage of all heart cells

Pioneering work in *C. elegans* established the importance of elucidating cell lineages to obtain a thorough understanding of animal development (Sulston and Horvitz, 1977). Our prior work has established the cell lineage of 10 out of the 16 heart cells that arise in each hemisegment of the posterior seven heart segments (Ward and Skeath, 2000). To define the lineage of the remaining heart cells, we used the FLP/FRT lineage tracing system (Struhl and Basler, 1993) to determine the lineal relationship of the two Eve-positive pericardial cells and four Tin-positive pericardial cells that arise in each hemisegment. This system creates random clones marked by *tau-lacZ* reporter gene activity. Briefly, we induced clones during stage 8 just as the pan-mesodermal divisions are being completed (Borkowski et al., 1995). This allowed us to induce clones in mesodermal cells prior to the emergence of heart precursors. To identify the lineage of Eve-positive pericardial cells we double labeled embryos for β-galactosidase to mark clones, and Eve to identify Eve-positive pericardial cells. To identify the lineage of Tin-positive pericardial cells we double labeled embryos for β-galactosidase to mark clones, and Tin to identify Tin-positive pericardial cells. In addition to the Tin-positive pericardial cells, Tin labels cardioblasts and Eve-positive pericardial cells. However, based on position and morphology one can unambiguously distinguish Tin-positive pericardial cells from Tin-positive cardioblasts and Eve-positive pericardial cells.

We identified eighteen clones that contained at least one Eve-positive pericardial cell. Eleven of these clones (61.1%) consisted solely of two Eve-positive pericardial cells (Fig. 1A), six clones (33.3%) consisted of two Eve-positive pericardial cells and one or two nearby heart or other mesodermal cells, and one clone (5.6%) consisted of a single Eve-positive pericardial cell. Thus, when we observe one Eve-positive pericardial cell within a clone of two or more cells a second Eve-positive pericardial cell always exists within this clone. These data demonstrate that the two Eve-positive pericardial cells within a hemisegment are siblings and arise from an Eve-positive pericardial cell precursor.

Our data on the lineage of Eve-positive pericardial cells contrasts with a prior lineage study (Park et al., 1998). This study also used the FLP/FRT lineage tracing system but determined that Eve-positive pericardial cells are not obligate siblings. We attribute the difference in our results to the different stages during which clones were induced in the two studies. We induced clones during stage 8, well before the division of Eve-expressing mesodermal cells during late stage 10. However,

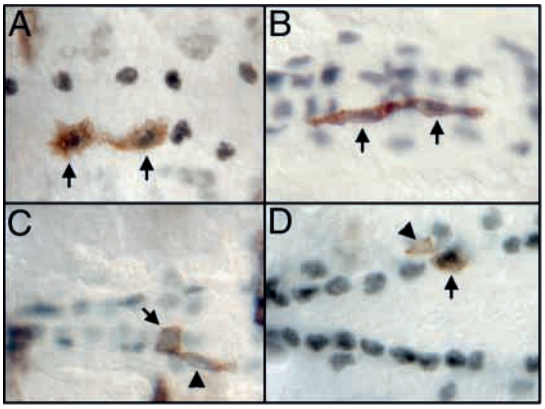

Fig. 1. Cell lineages of Eve- and Tin-positive pericardial cells and anterior Tin-positive cardioblasts. High-magnification dorsal views of stage 15-16 embryos labeled for β-galactosidase (brown) to identify clones and Eve (A) or Tin (B-D) (black). (A) Clone that contains two Eve-positive pericardial cells (arrows). (B) Clone that contains two Tin-positive pericardial cells (arrows). (C) Anterior heart clone that contains one Tin-positive cardioblast (arrow) and one Tin-positive pericardial cell (arrowhead). (D) Anterior heart clone that contains one Tin-positive cardioblast (arrow) and one Tin-negative pericardial cell (arrowhead). Anterior is towards the left.

Park et al. (Park et al., 1998) induced clones around stage 10, in close proximity to the time during which Eve-positive mesodermal cells divide. We speculate that the timing of *flp* induction in the prior study was too late to identify an obligate sibling relationship between Eve-positive pericardial cells. Our results agree with those of Carmena et al. (Carmena et al., 1998) who argue for a sibling relationship between Eve-positive pericardial cells based on gene expression studies.

Tin-positive pericardial cell clones fall into two classes: those that contained two Tin-positive pericardial cells (n=23), and those that contained one Tin-positive pericardial cell and one cardioblast (n=18). These two classes of clones arise in mutually exclusive regions of the heart. Clones that contain two Tin-positive pericardial cells arise in the posterior seven segments of the heart (we refer to this region as the posterior heart domain), whereas clones that contain one Tin-positive pericardial cell and one cardioblast arise anterior to this domain (we refer to this region as the anterior heart domain). The point of demarcation between these clonal types coincides precisely with the location of the first pair of Svp-positive cardioblasts (see below). These data demonstrate that heart cells exhibit distinct cell lineages as a function of position along the anteroposterior axis.

We identified a total of 24 Tin-positive pericardial cell clones in the posterior heart domain. Fifteen of these clones (62.5%) consisted solely of two Tin-positive pericardial cells (Fig. 1B), eight clones (33.3%) consisted of two Tin-positive pericardial cells and two nearby mesodermal cells, and one clone (4.2%) consisted of a single Tin-positive pericardial cell. Thus, when we observe one Tin-positive pericardial cell within a clone of two or more cells, a second Tin-positive pericardial cell always exists within this clone. These data indicate that the four Tin-positive pericardial cells found in each hemisegment of the posterior domain arise from two Tin-positive pericardial cell precursors. Our inability to identify any clones that contain four Tin-positive pericardial cells indicates that adjacent Tin-positive pericardial cell precursors are unlikely to share a common lineage.

We identified 18 Tin-positive pericardial cell clones in the anterior heart domain. All 18 clones consisted of one Tin-positive pericardial cell and one cardioblast (Fig. 1C). These data indicate that within this region Tin-positive pericardial cells arise from bi-potent heart precursors, each of which produces one Tin-positive pericardial cell and one cardioblast. These data also demonstrate that cardioblasts and Tin-positive pericardial cells in the anterior heart domain develop via a different cell lineage than cardioblasts and Tin-positive pericardial cells that develop in the posterior domain.

The analysis of ten additional cardioblast clones in the anterior heart domain support a distinct cell lineage for anterior versus posterior cardioblasts. Nine clones consisted of one cardioblast and one non-Tin-expressing pericardial cell (Fig. 1D), whereas a single clone consisted of two cardioblasts. Thus, most, if not all, anterior domain cardioblasts share a sibling relationship with a pericardial cell. In addition, all anterior domain cardioblasts exhibit cell lineages distinct from posterior domain cardioblasts. Together with the lineage data on Tin-positive pericardial cells, these results support the idea that cardioblasts and Tin-positive pericardial cells in the anterior heart domain carry out distinct functions from those found in the posterior heart domain.

Interestingly, the lineage of the twelve cardioblasts in the anterior heart domain appears fixed with respect to whether they share a sibling relationship with a Tin-positive or Tin-negative pericardial cell. We numbered these cardioblasts 1-12 from anterior to posterior with cardioblast 12 being immediately anterior to the first Svp-positive cardioblast. We identified four clones that contained cardioblast 12 and in each clone this cardioblast shared a sibling relationship with a Tin-negative pericardial cell. By contrast, cardioblasts 10 and 11 each share a sibling relationship with a Tin-positive pericardial cell (n=3/3 and 5/5 clones, respectively). We have not obtained multiple clones for all twelve cardioblasts; nonetheless, these data suggest a fixed relationship between the position of a cardioblast and whether its sibling pericardial cell expresses Tin. We speculate that the differences in gene expression between different pairs of sibling cardioblasts and pericardial cells in the anterior domain may reflect functional differences between such pairs of heart cells.

Loss of *pointed* function results in excess cardioblasts

We identified *pnt* as an inhibitor of cardioblast development in a screen for mutations that affect cardioblast and/or pericardial cell development. To identify genes that regulate heart development we screened ~2000 third chromosomal lethal P element lines obtained from the Hungarian P element Stock Collection for defects in the expression of Mef2 a protein expressed in all cardioblasts and Eve. We uncovered two P element mutations that cause an approximate twofold increase

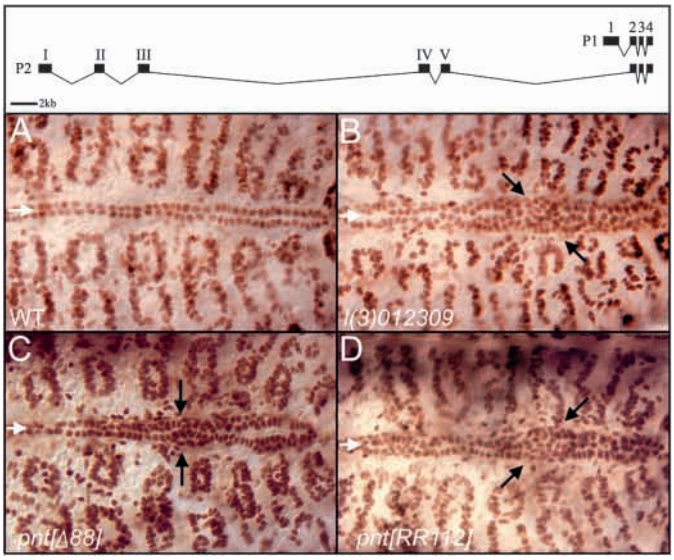

Fig. 2. *pointed* represses cardioblast development. (Top) The *pointed* locus, highlighting the intron-exon structure of *pntP1* and *pntP2*. (Bottom) High-magnification dorsal views of stage 16 wild-type (A), *l(3)012309* (B), $pnt^{\Delta 88}$ (C) and pnt^{RR112} (D) embryos labeled for Mef2. (A) In wild-type embryos, the heart is formed by two single rows of cardioblasts that meet at the dorsal midline (white arrow). In embryos that contain a P element insert in *pnt* (B), a deletion of the *pntP1* locus and the shared exons of *pntP2* (C) or a mutation in the splice donor site of a *pntP2*-specific exon (D), ectopic cardioblasts develop and form enlarged hearts comprising disorganized rows of cardioblasts (arrows, B-D). Anterior is towards the left; white arrow indicates the dorsal midline.

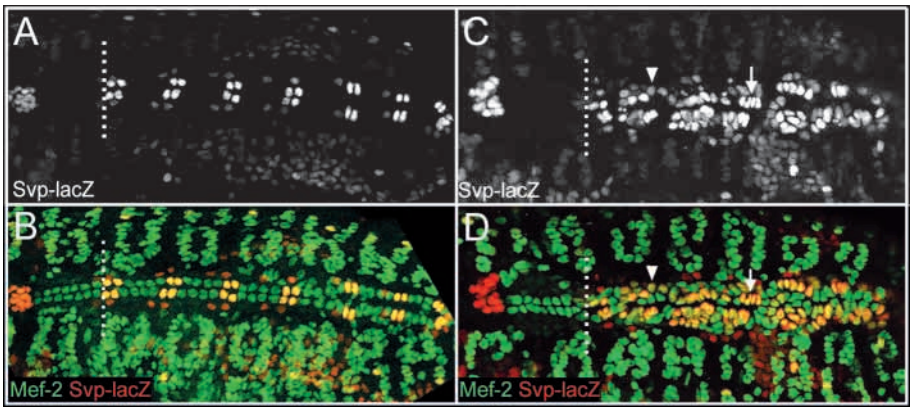

Fig. 3. *pointed* embryos exhibit a significant increase in Svp-positive cardioblasts. Dorsal views of stage 16 wild-type (A,B) and *pnt* (C,D) embryos labeled for *Svp-lacZ* (A,C), and *Svp-lacZ* and Mef-2 (B,D). (A,B) In wild-type embryos, 12 Svp-negative cardioblasts arise anterior to the first Svp-positive cardioblast (broken white line), seven of these cardioblasts are visible in A and B. Posterior to this location, there is a reiterative pattern of two *Svp-lacZ* positive cardioblasts (yellow/orange) and four *Svp-lacZ* negative cardioblasts (green) per hemisegment. (C,D) In *pnt* embryos, cardioblast development anterior to the first Svp-positive cardioblast (broken white line) appears normal. However, many ectopic cardioblasts are found posterior to this location and the majority of these cells express *Svp-lacZ* at high (arrow) or moderate levels (arrowhead). The broken white line separates the anterior heart domain from the posterior seven heart segments; anterior is towards the left.

in cardioblasts (Fig. 2; X. Tian and J.B.S., unpublished). One of these P elements [*l(3)S012309*] maps to cytological position 94F1-3 and was known to be an allele of *pnt* (FlyBase, 2003). To verify that lesions in *pnt* result in the formation of ectopic cardioblasts, we assayed the phenotype of five additional *pnt* alleles. Although the severity of the phenotype varies for each *pnt* allele, all alleles display a significant increase in cardioblast number relative to wild-type embryos (Fig. 2). With respect to the excess cardioblast phenotype, we can group these alleles into the following allelic series: $pnt^{S012309}$, $pnt^{2} > pnt^{RR112}$, $pnt^{RM254} > pnt^{\Delta 88}$, pnt^{07825}. The presence of excess cardioblasts in embryos homozygous mutant for each *pnt* allele indicates that *pnt* normally functions in heart development to repress cardioblast development.

Two distinct types of cardioblasts exist in the heart: Svp-positive cardioblasts and Tin-positive cardioblasts. To determine whether mutations in *pnt* result in an increase in one type of cardioblast or a general increase in all cardioblasts we assayed the relative percentage of the two types of cardioblasts in wild-type and *pnt* embryos. In wild-type embryos, a total of 52 cardioblasts develop per embryo side: 14 of these cardioblasts express *Svp-lacZ* and 38 express Tin but not Svp. In $pnt^{S012309}$ embryos an average of 98.5 cardioblasts develop per embryo side (n=10): 58.6 express Svp (a 318% increase relative to wild-type) and 41.3 express Tin but lack Svp (a 8.6% increase relative to wild-type). In $pnt^{S012309}/pnt^{2}$ embryos, an average of 99 cardioblasts develop per embryo side (n=5): 53 express *Svp-lacZ* (a 278% increase) and 46 express Tin but lack Svp (a 21% increase). Thus, the *pnt* excess cardioblast phenotype arises predominantly from an increase in Svp-positive cardioblasts.

Our analysis of heart development in *pnt* embryos indicated that the effect of *pnt* on cardioblast development is region specific. In wild-type embryos 12 cardioblasts develop anterior to the first pair of Svp-positive cardioblasts on each side of the embryo. As detailed in our lineage studies, these cardioblasts define the anterior heart domain. Interestingly, cardioblast development in the anterior domain is essentially normal in *pnt* mutant embryos (Fig. 3). In $pnt^{S012309}$ and in $pnt^{S012309}/pnt^{2}$ embryos, an average of 10.8 (n=10) and 12.4 (n=5) cardioblasts develop anterior to the first pair of *Svp-lacZ*-positive cardioblasts. Thus, in *pnt* embryos the ectopic cardioblast phenotype is restricted to the region of the heart, the posterior domain, that normally contains endogenous *Svp-lacZ*-positive cardioblasts.

To investigate whether *pnt* promotes pericardial cell development, we followed pericardial cell and lymph gland development in *pnt* embryos. In wild-type embryos, we detect 60.1 pericardial cells per embryo side (n=17) while in $pnt^{S012309}$ embryos we observe 31.4 pericardial cells per side (n=18; Fig. 4). All other *pnt* alleles exhibit significant reductions in pericardial cell number (not shown). We observe no effect of *pnt* on pericardial cell or lymph gland development in the anterior heart domain. Together with the data on cardioblast development, these results reveal that loss of *pnt* causes reciprocal effects on cardioblast versus pericardial cell

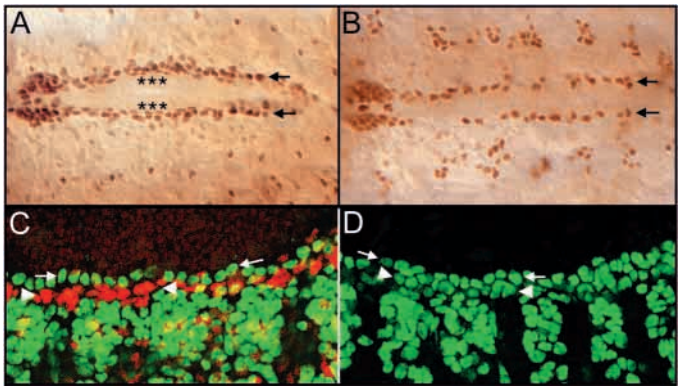

Fig. 4. *pointed* promotes pericardial cell development. Dorsal (A,B) and high magnification lateral (C,D) views of stage 16 (A,B) and early stage 13 (C,D) wild-type (A,C) and *pnt* (B,D) embryos labeled for ZFH1 to mark pericardial cells (A-C; red in C) and Mef2 (C,D; green). (A) In wild-type embryos, two bilateral stripes of pericardial cells (arrows) develop lateral to the cardioblasts (position of cardioblasts indicated by asterisks). (B) *pnt* embryos exhibit a severe reduction in pericardial cell number (arrows). (C) In early stage 13 wild-type embryos, pericardial cells (red cells; arrowheads) develop ventral and slightly interior to cardioblasts (green cells; arrows). (D) In early stage 13 *pnt* embryos, ectopic cardioblasts (arrowheads) arise in the location normally occupied by pericardial cells just ventral to the position of the endogenous cardioblasts (arrows). Anterior is towards the left.

development and that these effects are restricted to the posterior heart domain.

The reciprocal effect *pnt* has on the development of cardioblasts versus pericardial cells suggests that *pnt* may normally function during heart development to repress the cardioblast fate in cells destined to acquire the pericardial cell fate. To test this model, we carefully followed cardioblast development in *pnt* embryos. In wild-type embryos, all pericardial cells become detectable by late stage 12/early stage 13 in a position just ventral and slightly interior to cardioblasts (Fig. 4). At this stage and all subsequent stages, cardioblasts are clearly distinguished as a single line of cells at the dorsal most extreme of the mesoderm. In *pnt* embryos by late stage 12/early stage 13 we observe a clear excess of cardioblasts many of which are found in locations normally occupied by pericardial cells (Fig. 4). These results are consistent with a model in which *pnt* represses cardioblast development in presumptive pericardial cells thereby promoting pericardial cell development.

Owing to the specific increase in *Svp-lacZ* cardioblasts in *pnt* embryos, we also performed a detailed analysis of the development of *Svp-lacZ* cardioblasts and pericardial cells. In wild-type embryos, two *Svp-lacZ* heart precursors arise in each hemisegment during stage 11 (Ward and Skeath, 2000). Each precursor divides during stage 12 to yield one *Svp-lacZ* cardioblast and one *Svp-lacZ* pericardial cell. In *pnt* embryos the formation and division of each endogenous *Svp-lacZ* heart precursor is normal and wild-type numbers of *Svp-lacZ* pericardial cells persist throughout embryogenesis (data not shown). Thus, *Svp-lacZ* pericardial cells appear to develop normally in *pnt* embryos. However, we observe ectopic *Svp-lacZ* cardioblasts during late stage 12/early stage 13 in *pnt* embryos and these cells are found in locations normally occupied by pericardial cells (Fig. 4; not shown). These results, together with those detailed above, suggest that *pnt* normally functions in presumptive non-*Svp-lacZ*-expressing pericardial cells to repress the development of the *Svp-lacZ* cardioblast fate.

Our quantification of cardioblasts and pericardial cells in *pnt* embryos suggests the excess cardioblast phenotype does not arise solely from a conversion of pericardial cells into cardioblasts, as we observe a net loss of ~30 pericardial cells and a net gain of ~50 cardioblasts per embryo side. To investigate whether loss of *pnt* affects the proliferative potential of heart cells, we created and analyzed cardioblast clones in *pnt* embryos. We identified 124 clones in *pnt* embryos that contained at least one cardioblast. 97 clones (78%) consisted of either two cardioblasts or one cardioblast and one pericardial cell; 21 (17%) clones consisted of two cardioblasts and one or two pericardial cells whereas two (1.6%) consisted of one cardioblast. These clone types as well as their frequencies are similar to that observed for cardioblast clones in wild-type embryos (Ward and Skeath, 2000) (data not shown). However, in addition to these clones, we identified four (3.2%) that consisted of between six and 12 cardioblasts. We have never observed clones of more than four cardioblasts in wild-type embryos (n>200 clones). These data suggest that loss of *pnt* leads to a slight but perceptible increase in the proliferative capability of cardioblast precursors. However, the weak increase in cardioblast proliferation and the apparent conversion of pericardial cells into cardioblasts still appear insufficient to account for the approximate twofold increase in cardioblasts in *pnt* embryos. We hypothesize that loss of *pnt* also causes other dorsal mesodermal cells to acquire the cardioblast fate inappropriately. Consistent with this, we observe loss of specific dorsal muscles in *pnt* embryos.

pointed may regulate cardioblast development independently of the Ras pathway

Through the use of alternative promoters, the *pnt* locus encodes two distinct protein isoforms: PntP1 and PntP2. Both isoforms act as effectors of the Ras/MAP kinase pathway in multiple developmental contexts (Brunner et al., 1994; Klambt, 1993; O'Neill et al., 1994). This raises the possibility that the role of *pnt* during heart development is mediated through Ras/MAP kinase activity. Thus, we examined whether loss or reduction in the function of different members of the Ras/MAP kinase pathway also increased cardioblast number. We assayed cardioblast development in homozygous embryos singly mutant for *spitz*, *Star*, *rhomboid*, *heartless* and *heartbroken*. We also assayed cardioblast number in embryos in which we expressed dominant-negative forms of *ras* as well as the EGF- and *FGF*-receptors specifically in the mesoderm to reduce the activity of these genes in this tissue (see Materials and Methods). In all genetic backgrounds tested, we never observed an increase in cardioblast number. For the experiments involving dominant-negative constructs, we verified dominant-negative activity of the expressed protein by assaying *ras*-dependent developmental events that occur in the mesoderm prior to the role of *pnt* in cardioblast development. In all cases, the *ras*-dependent developmental events were perturbed (data not shown). Thus, we are confident that our failure to observe an effect on cardioblast number is not simply due to an inability of the dominant-negative proteins to inhibit the function of the targeted proteins in a timely manner. We interpret these results to suggest that *pnt* may regulate cardioblast development in a Ras-MAP kinase-independent manner.

PointedP2 regulates cardioblast number

The presence of two Pnt isoforms raises the question as to whether PntP1 and/or PntP2 carry out the function of the *pnt* locus during heart development. To address this issue, we used isoform-specific RNAi and isoform-specific rescue of the *pnt* cardioblast phenotype. We first generated double-stranded RNA probes to the unique 5′ regions of the PntP1 and PntP2 transcripts, and injected these separately into presynctial stage *Drosophila* embryos. We then labeled all such embryos either for Mef2 (to follow cardioblast development) or Mef2 and PntP1 protein (to follow cardioblast development and PntP1 protein levels). Embryos treated for *pntP1* RNAi exhibit severe morphological defects and a complete loss of PntP1 protein expression. In many embryos the extent of the morphological defects preclude a clean analysis of cardioblast development; however, it is possible to score cardioblast number in a subset of these embryos. We only scored cardioblast number in embryos devoid of detectable PntP1 protein. In these embryos, we observe an average of 53.2 cardioblasts per embryo side (n=11), nearly identical to the 52 cardioblasts that develop on each side of wild-type embryos. These results suggest that *pntP1* does not play a significant role in the regulation of cardioblast number by *pnt*.

By contrast, PntP2-RNAi indicates that *pntP2* function is

necessary to regulate cardioblast number. Embryos treated for PntP2 RNAi exhibit wild-type morphology, a clear excess of cardioblasts and an essentially normal pattern of PntP1 expression (Fig. 5). In these embryos, we observe an average of 80.1 cardioblasts per embryo side (n=22; ranging from 62 to 108 cardioblasts). The most severe *pntP2* RNAi phenotypes are as severe as those observed for pnt^{2} or $pnt^{S012309}$ embryos. We attribute the variable expressivity of the *pntP2* RNAi phenotype to the technique of RNAi as we observe a large variance in expressivity of the RNAi phenotype for all genes we have assayed in this manner.

Allele sequencing of pnt^{RR112} supports the idea that the PntP2 isoform is necessary to regulate cardioblast number. pnt^{RR112} is an allele of *pnt* we identified in an EMS screen to identify genes that control CNS and heart development. We find that pnt^{RR112} contains a molecular lesion that converts a G to A at the splice donor site immediately 3′ to the PntP2 specific fourth exon (converting the GT site to AT). This lesion should disrupt splicing of *pntP2* but not *pntP1*. Consistent with this, PntP1 expression is normal in pnt^{RR112} embryos. pnt^{RR112} embryos exhibit a strong excess cardioblast phenotype, indicating that the PntP2 isoform regulates cardioblast development (Fig. 2).

We also addressed the relative roles of *pntP1* and *pntP2* by assaying the effect generalized mesodermal expression of each *pnt* isoform has on cardioblast development in wild-type and *pnt* embryos. In these experiments, we used the Twist-GAL4 driver line to drive either *pntP1* or *pntP2* under UAS control throughout the mesoderm of homozygous wild-type or $pnt^{S012309}$ embryos. We find that mesodermal expression of *pntP2* in *pnt* embryos is sufficient to rescue to wild-type the *pnt* cardioblast phenotype (Fig. 5). In addition, we find that mesodermal expression of *pntP2* in otherwise wild-type embryos has no effect on cardioblast development (not shown). By contrast, we find that mesodermal expression of *pntP1* in wild-type or *pnt* embryos leads to a near complete loss of all cardioblasts and pericardial cells (Fig. 5). This drastic effect of *pntP1* on heart development may arise because of an effect of *pntP1* overexpression on early steps of mesodermal development prior to heart cell development. This possibility makes interpretation of whether *pntP1* can rescue the *pnt* cardioblast phenotype difficult. Nonetheless, these experiments clearly show that *pntP2* is sufficient to rescue the *pnt* heart phenotype. Together with the RNAi experiments and the phenotypic analysis of a *pntP2*-specific allele, these results demonstrate that *pntP2* is necessary and sufficient for the cardioblast and pericardial cell development, and suggest that *pntP1* is irrelevant in this developmental context.

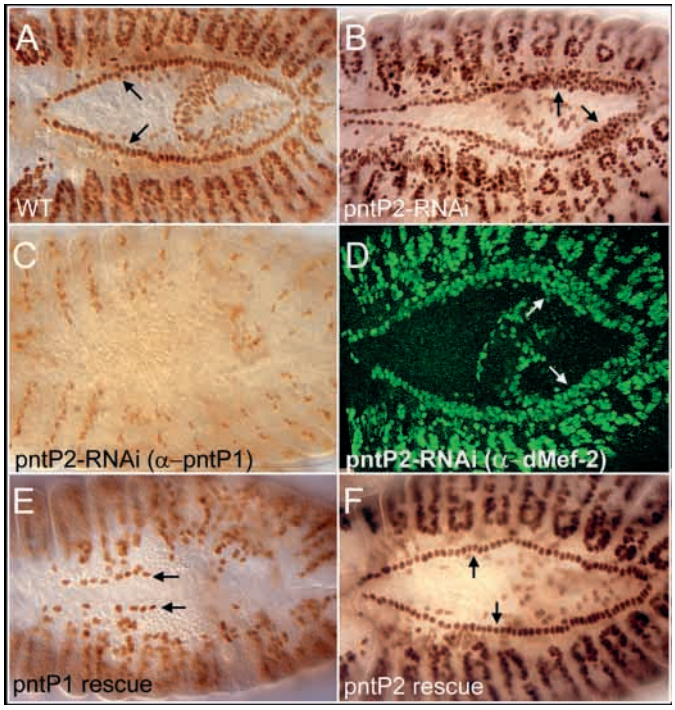

Fig. 5. PointedP2 is necessary and sufficient to repress cardioblast development. Dorsal whole heart views of stage 15 wild-type (A), PntP2 RNAi embryos (B-D) and pnt^{012309} embryos in which either *pntP1* (E) or *pntP2* (F) was expressed throughout the mesoderm labeled for Mef2 (A,B,D-F) or PntP1 (C). (A) Wild-type embryo showing the two bilateral rows of cardioblasts (arrows). (B) PntP2 RNAi-treated embryo exhibiting a significant increase in cardioblasts (arrows). (C,D) *pntP2* RNAi-treated embryo double-labeled for *pntP1* (C) and Mef2 (D). This embryo expresses PntP1 in essentially a wild-type pattern (C) and exhibits a significant increase in cardioblasts (arrows, D). (E) pnt^{012309} embryo in which *pntP1* has been expressed ubiquitously throughout the mesoderm exhibits a drastic loss of cardioblasts (arrows indicate cardioblasts). (F) pnt^{012309} embryo in which PntP2 has been expressed ubiquitously throughout the mesoderm exhibits wild-type cardioblast development (arrows). Anterior is towards the left.

pannier acts as a general promoter of dorsal mesoderm development

The published heart phenotype of the GATA transcription factor *pnr* is opposite to that of *pnt*. In *pnr* mutant embryos, too many pericardial cells and too few cardioblasts are thought to develop (Gajewski et al., 1999). As a first step towards examining the potential regulatory interactions between *pnr* and *pnt*, we carried out a detailed analysis of heart development in *pnr* mutant embryos. We used pnr^{VX6}, a null allele that contains a small deletion that removes all but the N-terminal nine amino acids of *pnr* (Ramain et al., 1993), as well as pnr^{1}, a molecularly uncharacterized allele. In contrast to a prior study, we find a loss of both cardioblasts and pericardial cells in *pnr* embryos (Fig. 6). We quantified the dorsal mesodermal phenotypes for Eve-positive pericardial cells as well as for all pericardial cells using the pan-pericardial marker Zfh1. In wild-type embryos we observe an average of 22.7 Eve-positive pericardial cells (n=32) and 61.1 Zfh1-positive pericardial cells (n=17) per embryo side. pnr^{VX6} embryos exhibit the most severe effect with an average of 9.4 (n=11) and 16.9 (n=21) Eve- and Zfh1-positive pericardial cells, respectively. pnr^{VX6}/pnr^{1} embryos exhibit an intermediate phenotype with an average of 16.4 Eve-positive pericardial cells (n=25) and 27.4 Zfh1-positivepericardial cells (n=18), while pnr^{1} embryos exhibit the mildest phenotype with an average of 21.2 and 37.4 Eve- (n=10) and Zfh1- (n=11) positive pericardial cells, respectively. We also observed a severe loss of cardioblasts and Odd-positive pericardial cells in these backgrounds although we did not quantify these phenotypes. The loss of cardioblasts and Odd-positive pericardial cells is most severe in pnr^{VX6} embryos and least severe in pnr^{1} embryos where short stretches

of cardioblasts are still visible (Fig. 6). These results indicate that *pnr* normally functions to promote the development of all heart cells.

Based on these results, we used Tin expression to determine the earliest stage at which we could identify a defect in dorsal mesoderm development in *pnr* embryos. In wild-type embryos, Tin expression becomes restricted to the dorsal mesoderm by stage 10 (Azpiazu and Frasch, 1993). During stage 11, Tin expression resolves to two stripes of cells: a dorsal stripe that labels the cardiac mesoderm and a more ventral undulating stripe that labels the primordia of the visceral mesoderm (Fig. 6) (Azpiazu and Frasch, 1993). In *pnr* embryos, Tin expression is normal until stage 11. However, during stage 11 Tin expression is lost from the cardiac mesoderm while it is maintained normally in the visceral mesoderm (Fig. 6). These results demonstrate that the earliest manifestation of cardiac mesoderm development is defective in *pnr* embryos. Furthermore, they suggest that the general lack of heart cells in *pnr* embryos arises indirectly via a defect in the specification of the cardiac mesoderm.

The above results indicate that pnr^{1} is a hypomorphic allele. Sequence analysis identified a single mutation in the pnr^{1}-coding region that converts a tryptophan residue at amino acid 180 to a premature stop codon roughly halfway through the first zinc finger. Using an antibody specific to epitopes N-terminal to this premature stop codon (Herranz and Morata, 2001), we find that the pattern and level of the mutant Pnr^{1} protein in homozygous pnr^{1} embryos are identical to those of the wild-type Pnr protein. However, while wild-type Pnr protein localizes predominantly to the nucleus, we find that Pnr^{1} protein localizes predominantly to the cytoplasm (not shown). These data together with the mild pnr^{1} phenotype relative to the pnr^{VX6} null allele suggest that the truncated Pnr^{1} protein retains residual activity.

pannier acts upstream of *pointed* in a developmental pathway

Our studies on *pnr* and *pnt* suggest these genes act in a developmental pathway in which the prior function of *pnr* to promote cardiac mesoderm formation is required for the subsequent action of *pnt* to specify between pericardial cell and cardioblast fates. If this model is correct, *pnr pnt* double mutants should display the *pnr* phenotype, as neither pericardial cells nor cardioblasts will arise in the absence of cardiac mesoderm. Consistent with this, pnr^{VX6} $pnt^{S012309}$ embryos lack cardioblasts and pericardial cells, and appear

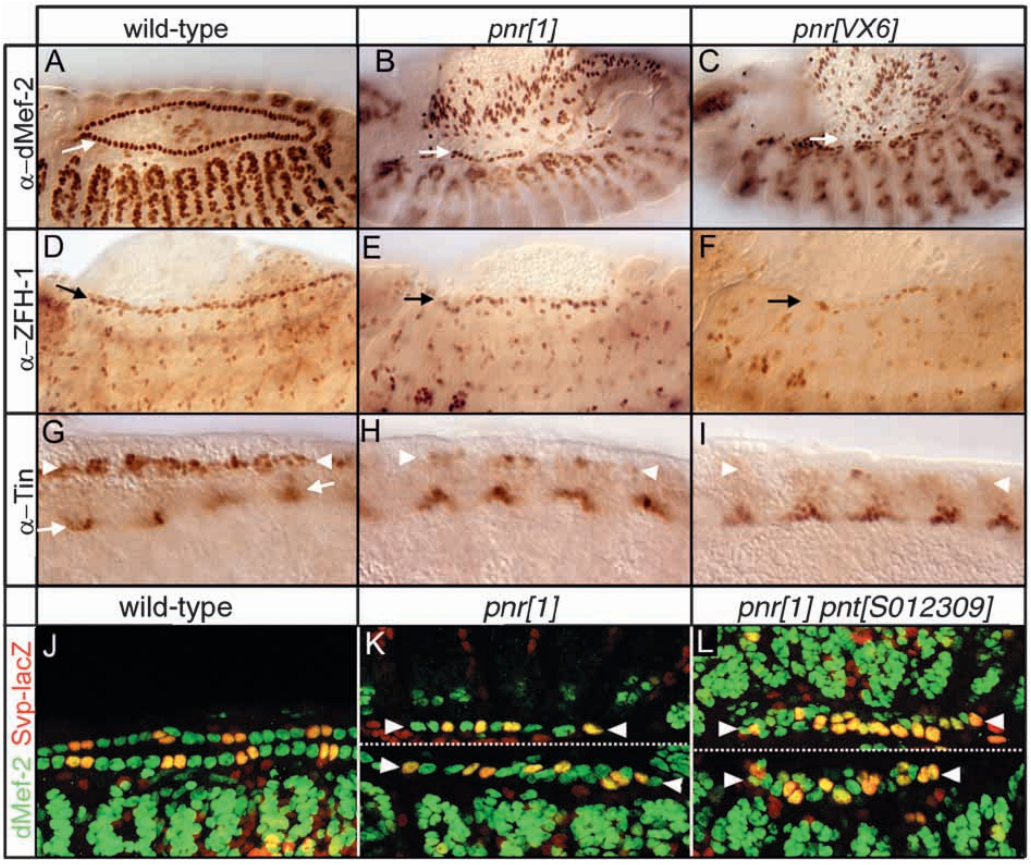

Fig. 6. *pannier* promotes the development of all heart cells. Lateral views of stage 15 (A-F) and stage 11 (G-I) embryos as well as high-magnification dorsal views of stage 16 (J-L) embryos of the indicated genotypes labeled for the indicated proteins. (A) Wild-type embryo showing two bilateral rows of cardioblasts (arrow). (B) In pnr^{1} embryos, most cardioblasts do not develop, although short stretches of cardioblasts still arise in this background (arrow). (C) In pnr^{VX6} embryos, cardioblasts almost never develop (arrow indicates normal position of the cardioblast row). (D) Wild-type embryo showing one of the two bilateral rows of pericardial cells (arrow). (E) In pnr^{1} embryos, there is a strong decrease in pericardial cells (arrow). (F) pnr^{VX6} embryos exhibit a more severe loss of pericardial cells (arrow). (G) In wild-type embryos Tin expression marks the cardiac mesoderm (arrowheads) and the presumptive visceral mesoderm (arrows). In (H) pnr^{1} and (I) pnr^{VX6} embryos, Tin expression is almost completely absent from the cardiac mesoderm (arrowheads) but is essentially wild type in the visceral mesoderm. (J) Wild-type embryo labeled for Mef2 (green) and *Svp-lacZ* (red) showing the normal reiterative pattern of four *Svp-lacZ* negative cardioblasts and two *Svp-lacZ* positive cardioblasts per hemisegment. (K) pnr^{1} embryos retain the 2:1 ratio of *Svp-lacZ*-negative to *Svp-lacZ*-positive cardioblasts although the precise alignment of these cardioblasts is perturbed (arrowheads indicate cardioblasts). (L) pnr^{1} pnt^{012309} embryos exhibit localized overproduction of cardioblasts (arrowheads) and the majority of these cardioblasts express *Svp-lacZ* (yellow or orange cells). Broken white lines in K and L separate images taken from two different embryos of the indicated genotype. Anterior is towards the left.

phenotypically indistinguishable with respect to heart development from pnr^{VX6} embryos (not shown). To test our model more stringently, we assayed heart development in pnr^{1} $pnt^{S012309}$ embryos. We used pnr^{1} embryos because small regions of cardiac mesoderm develop in pnr^{1} embryos and these regions produce short strings of cardioblasts that maintain the wild-type 1:2 ratio of Svp-positive:Svp-negative cardioblasts (Fig. 6). We reasoned that if *pnr* and *pnt* act in a developmental pathway, then we should observe the *pnt* mutant phenotype in those regions of pnr^{1} $pnt^{S012309}$ embryos in which cardiac mesoderm develops. In agreement with this, we observe local overproduction of cardioblasts in pnr^{1} $pnt^{S012309}$ embryos and the vast majority of these cardioblasts are *Svp-lacZ* positive. These double mutant studies support the model that *pnr* acts upstream of *pnt* in a developmental pathway.

DISCUSSION

The results in this paper indicate that *pnr* and *pnt* act sequentially to regulate heart development (Fig. 7, bottom panel). *pnr* acts early in mesoderm development to enable the cardiac mesoderm to form. Subsequent to this event, *pnt* acts within the cardiac mesoderm to regulate the ability of cells to choose between the pericardial or cardioblast fate. In this context, *pnt* inhibits the development of the Svp-class of cardioblasts and appears to function independently of Ras/MAP kinase pathway activity.

The effect of *pnt* on heart development is restricted to the posterior seven heart segments where Svp cardioblasts normally develop. Interestingly, our lineage studies identify a clear difference in the cell lineage of cardioblasts that develop

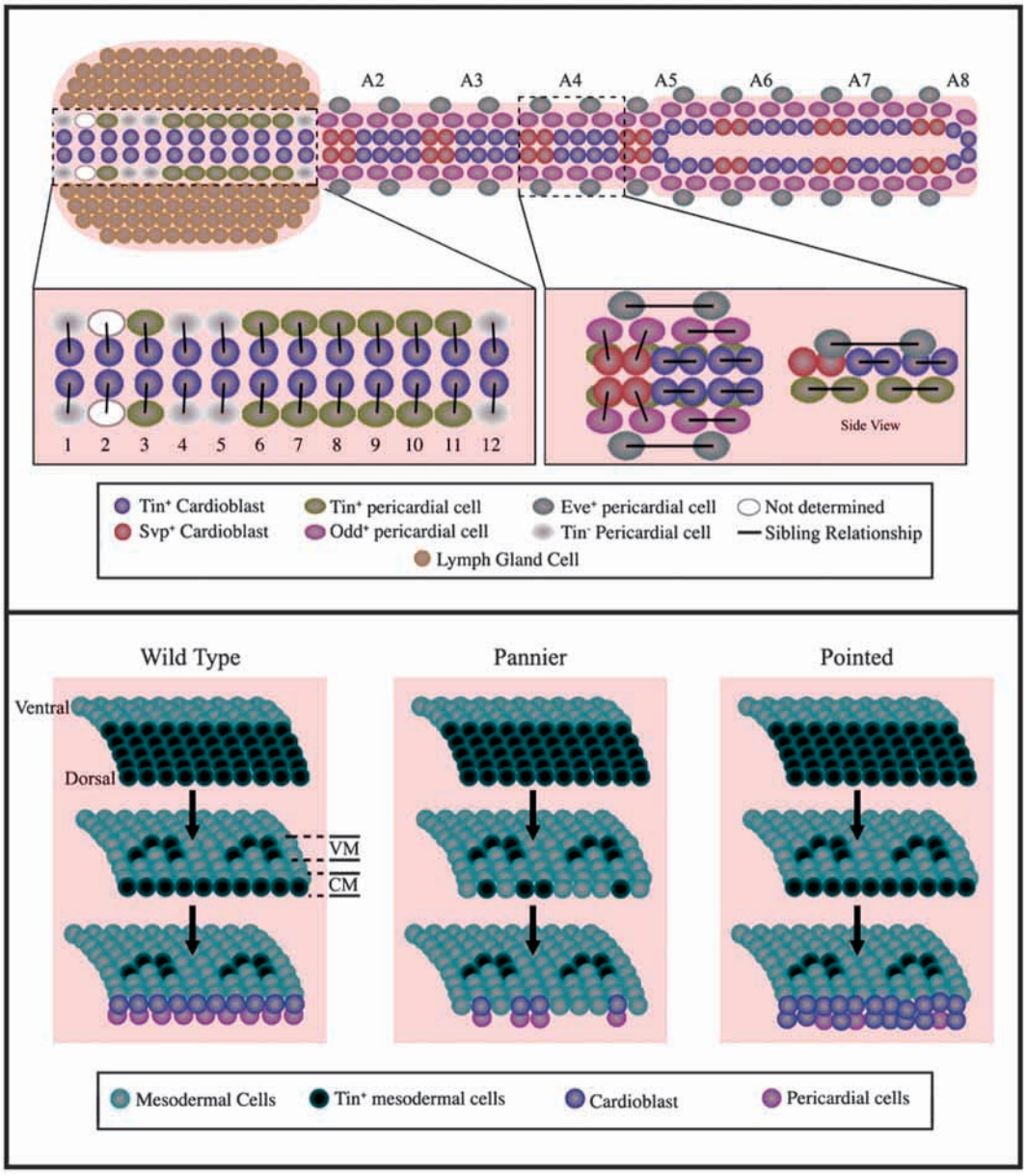

Fig. 7. Heart cells and their lineages, and a model for *pnt* and *pnr* function in the heart. (Top) The heart and heart cell lineages. In the whole heart schematic, Tin-positive pericardial cells are not shown in the posterior domain because in this region they reside beneath the cardioblasts. Segment names are provided above the schematic. The lineages of all anterior domain heart cells (left) and all heart cells found within one segment of the posterior heart domain (right) are shown below the whole heart schematic. Owing to sample size, Tin expression in pericardial cells 1-9 in the anterior domain should be considered preliminary. (Bottom) Cardioblasts and pericardial cells develop from the dorsalmost region of the mesoderm: the cardiac mesoderm (CM). Initially, all dorsal mesodermal cells express Tin (top). Tin expression then resolves into two stripes of cells: a dorsal stripe that defines the cardiac mesoderm and a ventral undulating stripe that labels the primordium of the visceral mesoderm (VM). As development proceeds, cardioblasts and pericardial cells develop from the cardiac mesoderm with pericardial cells residing interior and slightly ventral to cardioblasts. In the absence of *pnr* function, most of the cardiac mesoderm does not form; however, when cardiac mesoderm forms, the subsequent development of cardioblasts and pericardial cells is normal. In the absence of *pnt*, cardiac mesoderm forms normally but the subsequent development of pericardial cells is perturbed such that cardioblasts appear to develop in their place.

in the posterior seven heart segments versus those that develop more anteriorly (Fig. 7) (Ward and Skeath, 2000). These results identify a genetic and developmental distinction between these two regions of the heart. In addition, they suggest that cells in different regions of the heart carry out different functions and that these functions are probably under homeotic gene control. Future work that addresses the physiological role of these cells in heart function and the control of their development by homeotic genes should provide a more comprehensive understanding of heart development.

Does PntP2 act independently of the Ras/MAPK pathway?

Our data suggest that PntP2 may regulate cardioblast and pericardial cell development independently of Ras/MAP kinase activity. Given that every other developmental function of *pnt* has been traced back to receptor tyrosine kinase/Ras signaling activity, the apparent Ras independent activity of PntP2 is puzzling. As PntP2 is expressed broadly throughout the mesoderm (data not shown) (Klambt, 1993), a number of models can explain the apparent Ras-independent activity of PntP2 in the heart. For example, PntP2 may not require MAP-kinase-mediated phosphorylation to carry out a subset of its function. Consistent with this, phosphorylation of PntP2 does not appear to affect its DNA-binding ability (O'Neill et al., 1994). Thus, in the absence of MAP-kinase stimulation, PntP2 is still probably able to bind target promoters alone or in complexes with other proteins. Such an activity of PntP2 could on its own regulate target gene expression by blocking the ability of other transcriptional effectors to bind to and activate target gene transcription, or through an obligate association with other proteins required to activate (or to repress) target genes. Significant precedent exists for such activity. For example, the Su(H)/CSL and pangolin/TCF proteins are the transcriptional effectors of the *Notch* and *wingless* pathways, respectively, and in the absence of *Notch* or *wingless* activity these proteins can repress target gene transcription (Cavallo et al., 1998; Li et al., 1997; Mumm and Kopan, 2000; van de Wetering et al., 1997).

A second model is that PntP2 requires MAP kinase activation but that this activity is carried out by one of the other MAP kinase pathways in *Drosophila*: the JNK pathway or the p38 pathway. Preliminary phenotypic analyses indicate that heart development is normal in embryos mutant for *basket*, the *Drosophila* JNK-kinase (J.B.S., unpublished). Analysis of p38 kinase activity is presently limited because of the absence of suitable genetic backgrounds. A third possibility is that a novel Ras-dependent pathway does in fact activate PntP2 during heart development. This model is consistent with the recent identification of a novel receptor tyrosine kinase expressed in the developing visceral mesoderm (Loren et al., 2001). Our experiments that failed to identify a *pnt*-like excess cardioblast phenotype upon mesodermal overexpression of a dominant-negative form of Ras argue against this model. However, Ras is maternally loaded and it is extremely difficult to eliminate all Ras activity in this manner. Thus, even though we observed Ras-like mesodermal phenotypes in these experiments, we still may have missed a role for Ras in regulating cardioblast number because of differential sensitivity of different developmental pathways to partial Ras inactivation. Future work that (1) addresses the ability of MAP-kinase insensitive forms of PntP2 to regulate heart development, and (2) identifies PntP2 target genes in the heart and elucidates how PntP2 regulates such genes should help clarify the molecular basis through which PntP2 governs heart development.

Can Pannier function independent of its DNA binding ability?

Our phenotypic analysis of *pnr* conflicts with a prior study that showed an increase in pericardial cells in *pnr* mutants (Gajewski et al., 1999). This study used Eve to identify a subset of pericardial cells in pnr^{1} embryos. We attribute the difference in our results to our use of the pnr^{VX6} null allele, our ability to distinguish unambiguously Eve-positive pericardial cells from Eve-positive somatic muscle progenitors, and to specific defects in dorsal closure exhibited by *pnr* embryos that result in the local aggregation of cells in the dorsal region of the embryo. Our genetic results identify pnr^{1} as a hypomorphic allele and we find that Eve-positive pericardial cell formation is almost wild type in this background. In these experiments, we unambiguously identified Eve-positive pericardial cells via their co-expression of Zfh1 and were thus able to quantify precisely Eve-positive pericardial cell number in pnr^{1} embryos. This is important as one can observe local increases in Eve-positive mesodermal cells in *pnr* embryos. However, such apparent increases arise from the local aggregation of dorsal mesodermal cells in pnr^{1} embryos caused by defects in dorsal closure and not by an overall increase in Eve-positive mesodermal cells.

The genetic identification of pnr^{1} as a hypomorphic allele is intriguing given that molecular and expression analyses indicate the pnr^{1} lesion results from a premature stop codon in the middle of the first zinc finger and that the Pnr^{1} protein localizes predominantly to the cytoplasm. This lesion is expected to abrogate the DNA-binding ability of the Pnr protein. However, our genetic experiments indicate that the Pnr^{1} protein retains residual activity at least with respect to heart development. These results raise the possibility that Pnr may be able to carry out some of its functions independently of DNA binding. Precedence for such an activity comes from studies on a genetically engineered form of the homeodomain transcription factor Fushi-tarazu that lacks the homeodomain but retains significant biological activity (Copeland et al., 1996). Future work that focuses on a detailed structure function analysis of the Pnr protein should clarify whether Pnr can act independently of its DNA-binding ability in some developmental contexts.

We should also note that our *pnt* allelic series indicates that $pnt^{\Delta 88}$ exhibits a milder excess cardioblast phenotype than $pnt^{S012309}$, pnt^{2}, and pnt^{RR112}. This result is surprising as $pnt^{\Delta 88}$ deletes the exons *pntP2* shares with *pntP1* and as a result was assumed to be an amorphic allele of the *pnt* locus (Scholz et al., 1993). Using antisense RNA probes specific for the unique exons of *pntP2*, we observe an essentially wild-type pattern of *pntP2* transcription in $pnt^{\Delta 88}$ mutant embryos (data not shown). These data raise the possibility that the N-terminal regions of *pntP2* may also retain partial activity. Studies along the lines of those suggested for Pnr should also help elucidate whether truncated forms of PntP2 retain residual activity.

Do vertebrate ETS transcription factors regulate heart development?

As noted, significant similarity exists between the embryology and molecular regulation of early heart development in

Drosophila and vertebrates. In this context, the identification of a role for *pnt*, a member of the evolutionarily conserved ETS transcription factor family, in *Drosophila* heart development raises the possibility that ETS family proteins regulate vertebrate heart development. Consistent with this, ETS1 and ETS2, the two most closely related vertebrate ETS proteins to *pnt*, are expressed in the developing vertebrate heart; functional studies indicate these genes regulate the expression of specific genes in the heart (Majka and McGuire, 1997; Macias et al., 1998). However, knockout studies have not yet revealed a clear role for ETS1 or ETS2 in the morphological development or differentiation of the vertebrate heart. The existence of multiple vertebrate ETS-family members highly homologous to *pnt*, as well as a total of 25 ETS family members in humans suggests the possibility of functional redundancy in ETS protein function during vertebrate and mammalian heart development. Thus, a full understanding of ETS protein function during heart development awaits construction and analysis of animals multiply mutant for different ETS family members.

We are especially grateful to Manfred Frasch, Rolf Bodmer and Petra Levin for invaluable comments on the manuscript and various reagents. We are also indebted to Alan Michelson for providing many fly lines and helpful advice, and Scott Wheeler for Fig. 7. We thank Bruce Paterson, Gines Morata, Zhi-Chun Lai and the Developmental Studies Hybridoma bank for antibodies and/or fly stocks. As always we greatly appreciate the help received from Kathy Matthews and the Bloomington Stock Center. This work was supported by a grant to J.B.S. from NSF (IBN-0077727).

REFERENCES

Azpiazu, N. and Frasch, M. (1993). tinman and bagpipe: two homeo box genes that determine cell fates in the dorsal mesoderm of Drosophila. *Genes Dev.* **7**, 1325-1340.

Bodmer, R. and Frasch, M. (1999). Genetic determination of *Drosophila* heart development. In *Heart Development* (ed. N. Rosenthal), pp. 65-90. San Diego: Academic Press.

Borkowski, O. M., Brown, N. H. and Bate, M. (1995). Anterior-posterior subdivision and the diversification of the mesoderm in Drosophila. *Development* **121**, 4183-4193.

Brunner, D., Ducker, K., Oellers, N., Hafen, E., Scholz, H. and Klambt, C. (1994). The ETS domain protein pointed-P2 is a target of MAP kinase in the sevenless signal transduction pathway. *Nature* **370**, 386-389.

Carmena, A., Gisselbrecht, S., Harrison, J., Jimenez, F. and Michelson, A. M. (1998). Combinatorial signaling codes for the progressive determination of cell fates in the Drosophila embryonic mesoderm. *Genes Dev.* **12**, 3910-3922.

Cavallo, R. A., Cox, R. T., Moline, M. M., Roose, J., Polevoy, G. A., Clevers, H., Peifer, M. and Bejsovec, A. (1998). Drosophila Tcf and Groucho interact to repress Wingless signalling activity. *Nature* **395**, 604-608.

Copeland, J. W., Nasiadka, A., Dietrich, B. H. and Krause, H. M. (1996). Patterning of the Drosophila embryo by a homeodomain-deleted Ftz polypeptide. *Nature* **379**, 162-165.

Cripps, R. M. and Olson, E. N. (2002). Control of cardiac development by an evolutionarily conserved transcriptional network. *Dev. Biol.* **246**, 14-28.

FlyBase (2003). The FlyBase database of the Drosophila genome projects and community literature. *Nucleic Acids Res.* **31**, 172-175.

Frasch, M., Hoey, T., Rushlow, C., Doyle, H. and Levine, M. (1987). Characterization and localization of the even-skipped protein of Drosophila. *EMBO J.* **6**, 749-759.

Gabay, L., Scholz, H., Golembo, M., Klaes, A., Shilo, B. Z. and Klambt, C. (1996). EGF receptor signaling induces pointed P1 transcription and inactivates Yan protein in the Drosophila embryonic ventral ectoderm. *Development* **122**, 3355-3362.

Gajewski, K., Choi, C. Y., Kim, Y. and Schulz, R. A. (2000). Genetically distinct cardial cells within the Drosophila heart. *Genesis* **28**, 36-43.

Gajewski, K., Fossett, N., Molkentin, J. D. and Schulz, R. A. (1999). The zinc finger proteins Pannier and GATA4 function as cardiogenic factors in Drosophila. *Development* **126**, 5679-5688.

Herranz, H. and Morata, G. (2001). The functions of pannier during Drosophila embryogenesis. *Development* **128**, 4837-4846.

Jagla, K., Frasch, M., Jagla, T., Dretzen, G., Bellard, F. and Bellard, M. (1997). *ladybird*, a new component of the cardiogenic pathway in Drosophila required for diversification of heart precursors. *Development* **124**, 3471-3479.

Kennerdell, J. R. and Carthew, R. W. (1998). Use of dsRNA-mediated genetic interference to demonstrate that frizzled and frizzled 2 act in the wingless pathway. *Cell* **95**, 1017-1026.

Klaes, A., Menne, T., Stollewerk, A., Scholz, H. and Klambt, C. (1994). The Ets transcription factors encoded by the Drosophila gene pointed direct glial cell differentiation in the embryonic CNS. *Cell* **78**, 149-160.

Klambt, C. (1993). The Drosophila gene pointed encodes two ETS-like proteins which are involved in the development of the midline glial cells. *Development* **117**, 163-176.

Lai, Z. C., Fortini, M. E. and Rubin, G. M. (1991). The embryonic expression patterns of zfh-1 and zfh-2, two Drosophila genes encoding novel zinc-finger homeodomain proteins. *Mech. Dev.* **34**, 123-134.

Li, P., Yang, X., Wasser, M., Cai, Y. and Chia, W. (1997). Inscuteable and Staufen mediate asymmetric localization and segregation of prospero RNA during Drosophila neuroblast cell divisions. *Cell* **90**, 437-447.

Lilly, B., Zhao, B., Ranganayakulu, G., Paterson, B. M., Schulz, R. A. and Olson, E. N. (1995). Requirement of MADS domain transcription factor D-MEF2 for muscle formation in Drosophila. *Science* **267**, 688-693.

Lo, P. C. and Frasch, M. (2001). A role for the COUP-TF-related gene seven-up in the diversification of cardioblast identities in the dorsal vessel of Drosophila. *Mech. Dev.* **104**, 49-60.

Lo, P. C., Skeath, J. B., Gajewski, K., Schulz, R. A. and Frasch, M. (2002). Homeotic genes autonomously specify the anteroposterior subdivision of the Drosophila dorsal vessel into aorta and heart. *Dev. Biol.* **251**, 307-319.

Loren, C. E., Scully, A., Grabbe, C., Edeen, P. T., Thomas, J., McKeown, M., Hunter, T., Palmer, R. H. (2001) Identification and characterization of DAlk: a novel Drosophila melanogaster RTK which drives ERK activation in vivo. *Genes Cells* **6**, 531–544.

Macias, D., Perez-Pomares, J. M., Garcia-Garrido, L., Carmona, R. and Munoz-Chapuli, R. (1998). Immunoreactivity of the ets-1 transcription factor correlates with areas of epithelial-mesenchymal transition in the developing avian heart. *Anat. Embryol.* **198**, 307-315.

Majka, S. M. and McGuire, P. G. (1997). Regulation of urokinase expression in the developing avian heart: a role for the Ets-2 transcription factor. *Mech. Dev.* **68**, 127-137.

Mlodzik, M., Hiromi, Y., Weber, U., Goodman, C. S. and Rubin, G. M. (1990). The Drosophila seven-up gene, a member of the steroid receptor gene superfamily, controls photoreceptor cell fates. *Cell* **60**, 211-224.

Molina, M. R. and Cripps, R. M. (2001). Ostia, the inflow tracts of the Drosophila heart, develop from a genetically distinct subset of cardial cells. *Mech. Dev.* **109**, 51-59.

Mumm, J. S. and Kopan, R. (2000). Notch signaling: from the outside in. *Dev. Biol.* **228**, 151-165.

O'Neill, E. M., Rebay, I., Tjian, R. and Rubin, G. M. (1994). The activities of two Ets-related transcription factors required for Drosophila eye development are modulated by the Ras/MAPK pathway. *Cell* **78**, 137-147.

Park, M., Yaich, L. E. and Bodmer, R. (1998). Mesodermal cell fate decisions in Drosophila are under the control of the lineage genes numb, Notch, and sanpodo. *Mech. Dev.* **75**, 117-126.

Ramain, P., Heitzler, P., Haenlin, M. and Simpson, P. (1993). pannier, a negative regulator of achaete and scute in Drosophila, encodes a zinc finger protein with homology to the vertebrate transcription factor GATA-1. *Development* **119**, 1277-1291.

Scholz, H., Deatrick, J., Klaes, A., Klambt, C. (1993). Genetic dissection of pointed, a Drosophila gene encoding two ETS-related proteins. *Genetics* **135**, 455-468.

Skeath, J. B. (1998). The Drosophila EGF receptor controls the formation and specification of neuroblasts along the dorsal-ventral axis of the Drosophila embryo. *Development* **125**, 3301-3312.

Struhl, G. and Basler, K. (1993). Organizing activity of wingless protein in Drosophila. *Cell* **72**, 527-540.

Sulston, J. E. and Horvitz, H. R. (1977). Post-embryonic cell lineages of the nematode, Caenorhabditis elegans. *Dev. Biol.* **56**, 110-156.

van de Wetering, M., Cavallo, R., Dooijes, D., van Beest, M., van Es, J.,

Loureiro, J., Ypma, A., Hursh, D., Jones, T., Bejsovec, A. et al. (1997). Armadillo coactivates transcription driven by the product of the Drosophila segment polarity gene dTCF. *Cell* **88**, 789-799.

Ward, E. J. and Skeath, J. B. (2000). Characterization of a novel subset of cardiac cells and their progenitors in the Drosophila embryo. *Development* **127**, 4959-4969.